

Rotating smeared crack and orthotropic damage modeling for concrete

A.Sellier, B.Bary & B.Capra

Université de Marne la Vallée, Laboratoire de Génie et Urbanisme 2 rue A.Einstein 77420 Champs sur Marne

ABSTRACT: Induced anisotropy and anelastic strains of concrete are modeled within the general framework of the anisotropic damage mechanics. For this purpose, anisotropic criteria are developed and allow to govern crack growth in both direct and induced tension. In the case of induced tension, an original criterion traduces the effects of microscopic self-stresses generated at the aggregate-paste interfaces. The control of damage state is ensured by two 2nd order tensors, for direct and induced cracks. Damages are deduced from the cracking state by the theory of the weakest link, generalized to the non-radial loading cases by an original method inspired from the Weibull theory. This method allows to couple several non-coaxial cracking states. Although only cracks due to mechanical loading are taken into account in this study, the method can be easily extended to other kinds of degradation. To assess the relevance of the model, several numerical simulations are performed and analysed.

1 INTRODUCTION

The numerical prediction of concrete structures behavior is a field of study which has made important progress for these two last decades. Indeed, the increasing power of computers authorizes to improve reliability and accuracy in describing degradations and ruins risks. This improvement is deeply related to theoretical models, which have to reproduce with maximum of exactitude the pathological phenomena encountered on these structures. Among the great number of disorder causes (cracks due to mechanical loading, delayed strains due to shrinkage and creep, chemical attacks, ...), we only take into account in this study the reproduction of the concrete degradation subjected to mechanical loading, with the aim to carry out numerical simulations of structures behavior. However the model can be extended to other kind of fracture, thanks to a probabilistic formulation of the evolution laws and degradations coupling.

Several important phenomena must be taken into account to study the concrete behavior subjected to mechanical loading: cracking and its anisotropic aspects (inducing an anisotropic material behavior), unilateral behavior of the material (independence of stiffness in tension and compression), reproduction of anelastic strains (residual strains appearing after a total discharge of the structure). Numerous theoretical approaches are proposed to model the cracking phenomenon in concrete; the most widely accepted

are probably damage mechanics (Mazars et al. 1990, Fichant et al. 1997), fracture mechanics (Bazant et al. 1998, Tandon et al. 1995), and plasticity (Feenstra et al. 1995).

The model proposed in this study can be classified within the general framework of anisotropic damage mechanics, with reproduction of anelastic strains (Sellier et al. 1999). The cracks are assumed to initiate and propagate in mode I, and consequently bulk collapses and crack propagation in mode II or III are not described. Damages are represented by two 2nd order tensors associated with each type of cracking (direct or induced tension); the eigendirections of these tensors are able to rotate in the case of non-radial loading. This approach is already adopted by other authors (Mazars et al. 1990, Bary et al. 2000), and makes it possible to reproduce orthotropic cracks planes. The damage variables are deduced from the states of cracking by the Weibull theory (Weibull 1939) generalized in anisotropic media by an original method. The damage in tension is governed by a load function in effective stresses using a criterion of Rankine. In compression, induced crack states evolve according to a load function developed with the aim of taking into account self-stresses appearing at aggregate-paste interfaces. The anelastic strains are due to uncomplete reclosure of cracks after total discharge; their increases are coaxial with the effective stresses tensor and they can be partially closed by the effect of compressive stresses. In a finite element context, objectivity of

the model response in softening phase is ensured by the classical technique of Hillerborg (Hillerborg et al. 1976).

2 BASES OF THE MODEL

Cracks are assumed to propagate in concrete by the effect of microscopic effective stresses. The material behavior then becomes orthotropic and anelastic strains appear in the damage eigendirections. Both elastic response and anelastic strains changes are supposed completely determined by:

- the tensor of effective stresses noted $\overline{\overline{\sigma}}_{(R)}$
- the tensors of internal variables representing the cracking state, noted $\overline{\overline{Pf}}'_{(R)}$ for the cracks induced by tensile stresses and $\overline{\overline{Pf}}^c_{(R)}$ for the cracks induced by the compressive stresses (Sellier et al. 1999).

2.1 Stresses and strains

The effective stresses are linked to the apparent stresses by damage variables estimated in the eigendirections of effective stresses. These damage variables take into account the unilateral aspect of the concrete behavior by means of a partition of the stress tensor into positive and negative part equations (1) and (2).

This partition is carried out classically according to the sign of the eigenvalues of $\overline{\overline{\sigma}}_{(R)}$ (Mazars et al. 1990, Bary et al. 2000).

$$\overline{\overline{\sigma}}_{(R)} = \overline{\overline{\sigma}}'_{(R)} + \overline{\overline{\sigma}}^c_{(R)} \quad (1)$$

$$\begin{cases} \overline{\overline{\sigma}}'_{(\bar{\sigma}),I} = \overline{\overline{\sigma}}'_{(\bar{\sigma}),I} \left(1 - d^{+(\bar{\sigma}),11}(\overline{\overline{\sigma}}_{(R)}, \overline{\overline{Pf}}'_{(R)}, \overline{\overline{Pf}}^c_{(R)}) \right) \\ \overline{\overline{\sigma}}^c_{(\bar{\sigma}),I} = \overline{\overline{\sigma}}^c_{(\bar{\sigma}),I} \left(1 - d^{-(\bar{\sigma}),11}(\overline{\overline{\sigma}}_{(R)}, \overline{\overline{Pf}}'_{(R)}, \overline{\overline{Pf}}^c_{(R)}) \right) \end{cases} \quad (2)$$

The total strains result from the superposition of elastic and anelastic strains:

$$\overline{\overline{\varepsilon}}_{(R)} = \overline{\overline{\varepsilon}}^e_{(R)} + \overline{\overline{\varepsilon}}^a_{(R)} \quad (3)$$

The elastic strains are deduced from the effective stresses by a softening matrix, depending on the damage state and the current effective stresses:

$$\overline{\overline{d\varepsilon}}^e_{(R)} = \overline{\overline{H}}_{(R)} \left(E_0, \nu_0, \overline{\overline{Pf}}'_{(R)}, \overline{\overline{Pf}}^c_{(R)}, \overline{\overline{\sigma}}_{(R)} \right) \cdot \overline{\overline{d\sigma}}_{(R)} \quad (4)$$

The anelastic strains are subdivided in anelastic strains of tension and compression; in both cases they are function of the damage state, and of the current state of effective stresses which can reclose them partially in case of compression.

The eigenvalues of the apparent stress tensor are obtained from the eigenvalues of the effective stress tensor and the damages projected in the eigendirections of the effective stresses, by the expression:

$$\sigma_{(\bar{\sigma}),I} = \overline{\overline{\sigma}}'_{(\bar{\sigma}),I} (1 - d'_{(\bar{\sigma}),I}) + \overline{\overline{\sigma}}^c_{(\bar{\sigma}),I} (1 - d^c_{(\bar{\sigma}),I}) \quad (5)$$

The total strains are classically obtained by superposition of the elastic and anelastic strain:

$$\overline{\overline{\varepsilon}}_{(R)} = \overline{\overline{\varepsilon}}^e_{(R)} + \overline{\overline{\varepsilon}}^a_{(R)} + \overline{\overline{\varepsilon}}^c_{(R)} \quad (6)$$

To ensure, in finite element context, the objectivity of post peak dissipation in tension, the relation between effective stresses and elastic strains includes a Hillerborgh procedure in tension, the elastic behavior is then proposed by:

$$d\overline{\overline{\varepsilon}}^e_{(\bar{\sigma}),I} = \frac{1}{E_0} \left[H d\overline{\overline{\sigma}}'_{(\bar{\sigma}),I} + d\overline{\overline{\sigma}}^c_{(\bar{\sigma}),I} - \nu_0 \left\{ d\overline{\overline{\sigma}}'_{(\bar{\sigma}),II} + d\overline{\overline{\sigma}}'_{(\bar{\sigma}),III} \right\} \right] \quad (7)$$

with H the Hillerborgh term:

$$H = \left(\frac{l'_c}{l'_{(\bar{\sigma}),I}} + \left(1 - \frac{l'_c}{l'_{(\bar{\sigma}),I}} \right) \frac{(1 - \max[d'_{(\bar{\sigma}),I}, d'_{peak}])}{1 - d'_{peak}} \right) \quad (8)$$

The Hillerborgh procedure is applied to the elastic strain components coaxial to the eigendirections of the positive effective stresses. l'_c and $l'_{(\bar{\sigma}),I}$ are respectively the internal characteristic length for tension and the characteristic size of the finite element in the considered direction (Oliver 1989). The Hillerborgh procedure is not applied in compression.

2.2 Damage

Cracks are described by two 2nd order tensors noted respectively $\overline{\overline{Pf}}'_{(R)}$ for the cracks due to direct tension and $\overline{\overline{Pf}}^c_{(R)}$ for cracks consecutive to compressive stresses. The eigenvalues of these tensors represent normalized states of cracks, thus they vary from 0 for healthy material to 1 for completely degraded material. When considering a representative elementary surface of concrete, and taking into account the randomness of the place where cracking occurs, the measurement of normalized cracks as defined can be directly related to a probability of surface creation of discontinuity. This probabilistic definition of damage thereafter allow to deal with the problems of coupling between

various degradation causes on the one hand and the macroscopic damage on the other hand by using the theory of the weakest link (Sellier et al. 1999).

2.2.1 Damage in tension

Cracking in tension can be due either to direct tension stresses, or induced tension stresses caused by orthogonal compression. According to Weibull theory, the probability P_S corresponding to healthy surface is equal to the product of the probabilities P_S^t and $P_S^{c(\alpha_{ct})}$ corresponding respectively to healthy surface after being subjected to tensile stress and orthogonal compressive stress:

$$P_S = (P_S^t)(P_S^c)^{\alpha_{ct}} \quad (9)$$

In this expression, α_{ct} is the probabilistic weight of the compression cracks on the damage in tension; it is consequently a coupling coefficient between the cracks induced by compressive stresses and the damage in tension. In addition, the fact that a representative elementary surface can only be healthy or degraded involves the relation $P_f + P_s = 1$. The definitions of resulting damage (from coupling of different degradation causes) and both induced and direct tension cracks, together with equation (9) lead to the following relation:

$$(1 - d^t) = (1 - P_f^t)(1 - P_f^c)^{\alpha_{ct}} \quad (10)$$

For the nonradial loading paths, the expression (10) of the theory of the weakest link is not directly exploitable since the cracking tensors do not have their eigendirections confounded. This difficulty can be circumvented by applying to the preceding relation the transformation ϕ defined by:

$$X \xrightarrow{\phi} -\ln(1 - X) \quad (11)$$

Equation (10) becomes then:

$$\underbrace{-\ln(1 - d^t)}_{\delta^t} = \underbrace{-\ln(1 - P_f^t)}_{\beta^t} + \alpha_{ct} \underbrace{(-\ln(1 - P_f^c))}_{\beta^c} \quad (12)$$

δ is called damage index, β^t and β^c are denoted indices of cracking respectively by direct and induced tension. The transformation ϕ is applied to the eigenvalues of the tensors $\overline{P_f}$ to obtain the eigenvalues of the tensors $\overline{\beta}$. After having expressed all the tensors $\overline{\beta}$ in the same reference (R), the tensor of damage indices $\overline{\delta}$ is deduced by a simple linear combination of $\overline{\beta}$:

$$\overline{\delta}_{(R)} = \overline{\beta}_{(R)}^t + \alpha_{ct} \overline{\beta}_{(R)}^c \quad (13)$$

By application of the transformation ϕ^{-1} defined at equation (11), the eigenvalues of coupled damage tensors can be calculating by:

$$d'_{(\beta^t),I} = 1 - \exp(-\delta'_{(\beta^t),I}) \quad (14)$$

Taking into account the assumption of crack opening in mode I, we propose to express the indices of cracking thanks to a Weibull function in which an effective threshold stress is associated with each cause of cracking:

$$\beta'_{(\beta^t),I} = \frac{1}{m^i} \left(\frac{\tilde{\sigma}_{(\beta^t),I,SEUIL}^i}{\sigma_u^i} \right)^{m^i} \quad (15)$$

with $i = \{t \text{ for cracks due to direct tension, } c \text{ for cracks due to induced tension}\}$

σ_u^i characterizes the material cohesion and m^i the dispersion of cohesion. The higher m^i is, the more homogeneous and brittle the material is. The evolution of the threshold stress is governed by the progression of the load surface associated with each kind of cracking (Sellier et al. 1999).

2.2.2 Damage in compression

The damage in compression is due to the appearance of cracks parallel to the direction of compression. This condition is translated, thanks to the theory of the weakest link, in the following way for each eigendirection of the effective stress tensor:

$$(1 - d_t^c) = (1 - P_{II}^c)^{\alpha_{ic}} (1 - P_{III}^c)^{\alpha_{ic}} \times (1 - P_{II}^t)^{\alpha_{ic}} (1 - P_{III}^t)^{\alpha_{ic}} \quad (16)$$

In this expression, the coefficients α_{ic} are the probabilistic weights of the tension cracks on the damage in compression. The functions ψ describe crack reclosure, and vary between 1 for open cracks to 0 for closed cracks. The transformation ϕ defined by expression (11) can also be applied to the expression of the damage in compression (16). This transformation allows, as in the tension case, to simplify the coupling problem in an additive problem of cracking indices tensor.

2.3 Damage evolutions

2.3.1 Damage criteria

A load function f^s is defined for each cause of cracking:

$$f^s = \tilde{\sigma}_{(\overline{\beta}),I,EQU}^s - \tilde{\sigma}_{(\overline{\beta}),I,SEUIL}^s \text{ with } s = \{t, c\} \quad (17)$$

In this expression, $\tilde{\sigma}_{(\bar{\sigma}),I,EQU}^s$ is the equivalent effective stress, it depends on the state of current effective stress and gives the form of the cracking criterion. The flow and consistency conditions are written respectively by:

$$\begin{cases} df^s = 0 \\ f^s = 0 \end{cases} \text{ and } d\tilde{\sigma}_{(\bar{\sigma}),I,EQU}^s = d\tilde{\sigma}_{(\bar{\sigma}),I,EQU}^s \quad (18)$$

A Rankine criterion in each eigendirection of effective stress tensor is adopted for damage in tension, which leads to the following equivalent stress:

$$\tilde{\sigma}_{(\bar{\sigma}),I,EQU}^t = \langle \tilde{\sigma}_{(\bar{\sigma}),I} \rangle^+ \quad (19)$$

In compression, cracks initiate parallel to the directions of compression loading, in the neighborhood of aggregate - hydrated cement paste interfaces. This mode of initiation is due to the existence of self-stresses (figure 1) generated by the difference of stiffness between aggregate and cement paste.

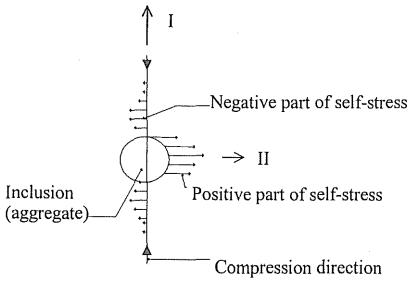


Figure 1. Self-stresses generated by compressive stresses.

If compression takes place in direction I, the effective stress in direction II sees its value varying locally around an average value. This effective stress in direction II is obtained by superposition of a state of average effective stress and a system of self-stresses, the positive part of which is located at aggregate - paste interfaces. This self-stresses is defined by a zero average and a non-zero standard deviation; a measurement of self-stresses is thus the standard deviation of the microscopic stress. We assume that this standard deviation is proportional to the orthogonal compressive stress. The following expression is then proposed for the equivalent stress characterizing the microscopic state of stress in the vicinity of the aggregate-paste interface:

$$\tilde{\sigma}_{(\bar{\sigma}),I,EQU}^c = \langle \tilde{\sigma}_{(\bar{\sigma}),II} \rangle^- + C \sqrt{\langle \tilde{\sigma}_{(\bar{\sigma}),I} \rangle^-^2 + \langle \tilde{\sigma}_{(\bar{\sigma}),III} \rangle^-^2} \quad (20)$$

In this expression, C is a coefficient allowing to control the aspect of load surface in the planes of the effective stresses. This coefficient fixes the intensity

of equivalent self-stresses in function of the orthogonal compressive stresses. C is thus all the higher as mechanical properties of aggregate and cement paste are different. It represents the heterogeneity of the concrete: the more C is, the less the concrete resists.

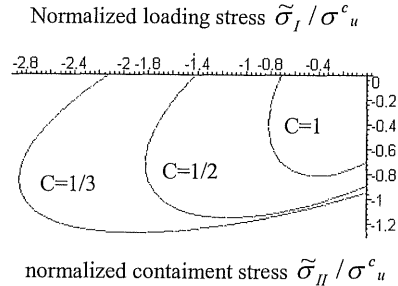


Figure 2. damage equipotentials d_i in function of normalized effective stresses e_t in plane stresses.

Figure 2 represents the curves of constant-damage of compression in the loading direction I. Both harmful effects of heterogeneities (resistance reduction due to the increase of C) and sensitivity of the compressive stress to a stress of containment in perpendicular direction are highlighted on this figure.

2.3.2 Coupled damages indices

The coupled damage indices are expressed according to equation (14) by:

$$\delta_{(\bar{\sigma}),I}^i = -\ln(1 - d_{(\bar{\sigma}),I}^i) \quad (21)$$

where $i=\{t$ if damage affects a stress eigenvalue in tension, c in the case of compression.

The macroscopic damage is obtained by applying the weakest link theory on the damages resulting from different causes:

$$\bar{\delta}_{(R)}^j = \sum_{k=1}^n \alpha_{kj} \bar{\delta}_{k(R)}^j \quad (22)$$

where α_{kj} are the coupling coefficients between cracks of origin k and the damage j , with $j=\{t$ for tension, c for compression. $\bar{\delta}_k^j$ is the marginal index j associated with cracks of origin k . The marginal damage indices $\bar{\delta}_k^j$ are obtained by a linear combination of the indices of cracking $\bar{\beta}$ as defined in equation (13). The marginal damage indices in tension are then expressed by:

$$\delta_{k(\beta)_I}^t = \psi_I^k \beta_I^k \quad (23)$$

In the same way, the marginal damage indices in compression are proposed in the following form to take into account induced cracks in direction II and III on damage in direction I :

$$\delta_{k(\beta^i)_I}^c = \psi_{II}^k \beta_{II}^k + \psi_{III}^k \beta_{III}^k \quad (24)$$

This last expression is equivalent to a weakest link formulation between directions II and III . In order to ensure evolution of damage coaxial to effective stress eigendirections, only the diagonal terms of the indices of cracking tensors $\overline{\beta}^i$ expressed in these eigendirections are affected. This procedure allows a possible rotation of the eigendirections of the tensors $\overline{\beta}^i$ if the eigendirections of these tensors are different from those of the effective stress tensor.

2.4 Anelastic strains

In tension as in compression, increments of anelastic strain are assumed to be coaxial to the increments of indices of cracking, consequently to the effective stresses. The increments of marginal anelastic strains (subscript 0) are defined independently of crack re-closure in the following form:

$$d\varepsilon_{(\bar{\sigma})_I}^{a,s,0} = df_{(\bar{\sigma})_I}^s \varepsilon_0^s \cdot P_{(\bar{\sigma})_I}^s \quad \text{with } s=\{t,c\} \quad (25)$$

In equation (25), $P_{(\bar{\sigma})_I}^s$ takes into account the Hillerborgh procedure on the anelastic strains in tension by the following expression:

$$P_{(\bar{\sigma})_I}^t = \frac{k}{l_{(\bar{\sigma})_I}} \quad (26)$$

In compression $P_{(\bar{\sigma})_I}^c = 1$. ε_0^s is an adjusting parameter obtained by a tensile test or from direct compression with cycles of load discharges. $f_{(\bar{\sigma})_I}^s$ is a function of damage state proposed in the following form:

$$f_{(\bar{\sigma})_I}^s = \frac{d_{(\bar{\sigma})_I}^{s,*}}{1 - d_{(\bar{\sigma})_I}^{t,*}} \quad \text{with } s=\{t,c\} \quad (27)$$

where :

$$d_{(\bar{\sigma})_I}^{s,*} = 1 - \exp\left(-\left\langle \beta_{(\bar{\sigma})_I}^s - \frac{1}{m^s} \right\rangle^+\right) \quad \text{with } s=\{t,c\} \quad (28)$$

The anelastic strains in tension as in compression can be partially closed by the effects of compressive stresses. The marginal anelastic strains defined in

equation (25) are then corrected using crack re-closure function ψ in the following way:

$$\varepsilon_{(\bar{\sigma}^{a,t})_I}^{a,t} = \psi_{(\bar{\sigma}^{a,t})_I}^t \varepsilon_{(\bar{\sigma}^{a,t})_I}^{a,t,0} \quad (29)$$

$$\varepsilon_{(\bar{\sigma}^{a,c})_I}^{a,c} = \left(\psi_{(\bar{\sigma}^{a,c})_I}^c \varepsilon_{(\bar{\sigma}^{a,c})_I}^{a,c,0} \right) - \nu_p \left(\psi_{(\bar{\sigma}^{a,c})_{II}}^c \varepsilon_{(\bar{\sigma}^{a,c})_{II}}^{a,c,0} + \psi_{(\bar{\sigma}^{a,c})_{III}}^c \varepsilon_{(\bar{\sigma}^{a,c})_{III}}^{a,c,0} \right) \quad (30)$$

The coefficient ν_p is measured on an uniaxial compression test on a cylindrical concrete specimen.

3 NUMERICAL SIMULATIONS

In this section are presented three studies which illustrate the response of the model.

3.1 Willam test

The Willam test consists firstly to impose on a single finite element an uniaxial increasing strain up to the peak of the behavior law; secondly, as soon as the peak is reached, the element is subjected to additional shearing and orthogonal tension strains (same rate for shearing, twice larger rate for tension). The second phase of the Willam test conducts to a rotation of both strains and stresses eigendirections, and for softening materials to a change of sign of the shear stress.

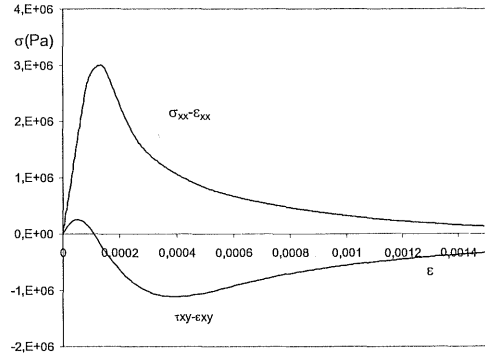


Figure 3: Numerical results of the Willam test in term of strain-stress curves.

Numerical results of the Willam test are presented on Figure 3 in term of strain-stress curves. Figure 4 shows that the orthotropic damage allows to reach the maximum tensile strength in orthogonal directions at two different moments. Moreover this figure illustrates the offset between rotations of respectively crack and stress tensor eigendirections.

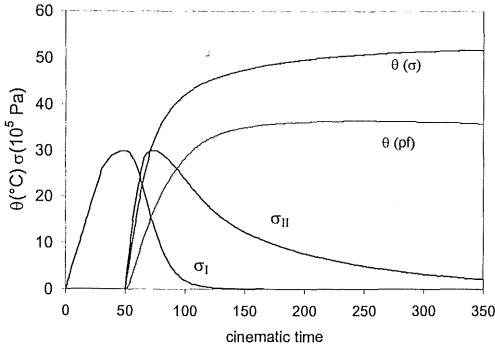


Figure 4 : Stress Eigenvalues σ_I and σ_{II} ; evolutions of the rotation angles of respectively stress tensor $\theta(\sigma)$ and damage tensor $\theta(pf)$ eigendirections.

3.2 Notched beams subjected to three points bending - Scale effect

The model response to three single-edged notched beams of different size subjected to three points bending is presented in this section. Numerical results are confronted with experimental ones provided by (Saouridis 1988) in term of loading strength versus mid-span displacement curves; in addition the scale effect of the three calculated beams is highlighted and compared to experimental data and to Bazant's law (Bazant et al. 1998). Dimensions of the beams are mentioned in Table 1 below. Young modulus is $E=32000\text{Mpa}$, Poisson ratio $\nu=0.2$ and tensile strength $f_t=3.8\text{MPa}$.

Table 1: geometric properties of the three beams

| | L(m) | h (m) | b (m) |
|--------|------|-------|-------|
| Small | 0.80 | 0.1 | 0.1 |
| Medium | 1.13 | 0.2 | 0.1 |
| Large | 1.38 | 0.3 | 0.1 |

Figure 5 represents the damage distribution on large beam (L) at the end of the calculation, in deformed configuration. The mesh in the vicinity of the notch is refined (8 elements) in order to capture damage initiation.

Figure 6 presents the loading strength versus mid-span vertical displacement curves, obtained numerically for the three beams; these results are compared to the experimental data. The confrontation be-

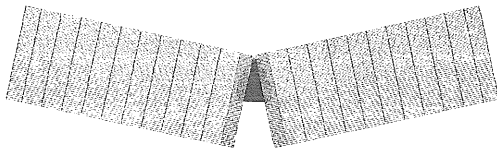


Figure 5: damage distribution on large beam (L) in deformed configuration.

tween the numerical and experimental results shows a very good prediction of the maximum loading force for the three beams, and a good description of their post-peak behavior.

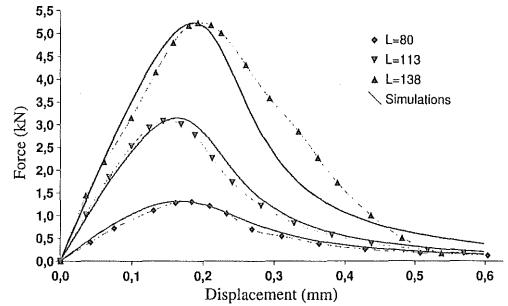


Figure 6: loading strength versus mid-span vertical displacement curves obtained numerically for the 3 beams (continuous lines); comparison with experimental results described in (Saouridis 88) (dotted lines + symbols).

The scale effect as restored by the model is presented on Figure 7 in term of nominal stress σ_N versus ratio height of the beam d / greatest dimension of aggregates d_a (equal to 8 mm). The resulting values are compared to experimental data and to Bazant's law of scale effect (Bazant et al. 1998, Mazars et al. 1994) giving the evolution of the nominal stress σ_N by:

$$\sigma_N = Bf_t \left(1 + \frac{1}{k_0} \frac{d}{d_a} \right)^{-1/2}$$

$k_0 = 20$ results from (Mazars et al. 1994); $B = 0.52$ was identified to correspond to the experimental value $f_t = 3.8 \text{ MPa}$ provided by (Saouridis 1988). According to Figure 7, numerical and experimental results are in very good agreement. The internal length parameter of the model, whose value is fixed here to 27 mm, appears to correctly describe the scale effect of structures.

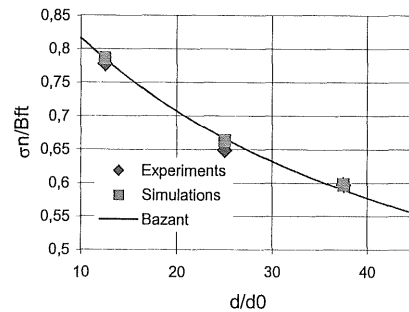


Figure 7 : scale effect study; numerical results are compared to experimental ones (Saouridis 1988) and to the Bazant's law (Bazant et al. 1998).

3.3 Single-notched beam subjected to fracture in mixte bending – shearing mode

The beam studied here presents a geometry knows as “Iosipescu” type (Schlangen 1993). Loading apparatus and geometry are presented on Figure 8; both metal plates of loading and loading bandage are included in the mesh.

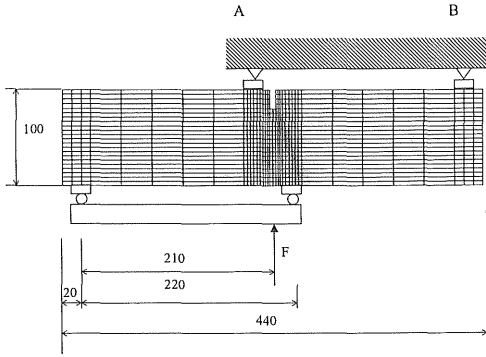


Figure 8 : mesh properties; loading and boundary conditions, and damage pattern at final step calculation.

Data concerning concrete are: Young modulus 35000MPa, Poisson coefficient 0.2, tensile strength 3.0Mpa, fracture energy 0.12 N/mm.

The examination of damage tensors eigendirections near the notch reveals the existence of strong distortions, which indicates a high level of damage in two orthogonal directions. Further from the notch, only one principal value is significant, which means that rotations of stresses are moderate in this zone. The crack thus opens in mixed mode near the notch and in mode I in the opposite side of the notch.

The damage distribution represented in Figure 8 shows that the crack initiates obliquely in respect to the notch, then turns towards the external edge of the metal plate used as loading support. This mode of crack propagation is in good agreement with experimental observations (Schlangen 1993). The main crack is very localized and does not follow the mesh; it is ranged by a diffuse cracking zone where the

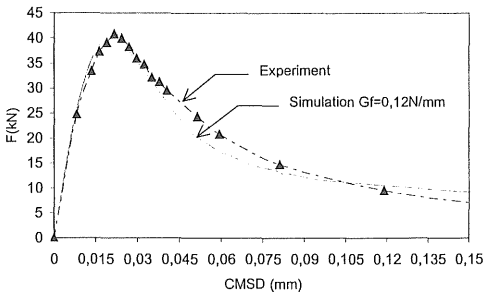


Figure 9 : Calculated and experimental curve CMSD

damage does not reach the peak value of the behavior law in direct tension. The crack mouth shearing displacement (CMSD) is compared to the experimental data resulting from (Schlangen 1993) on Figure 9; this confrontation shows a good description of the peak load and the structure behavior.

4 CONCLUSION

This study presents a theoretical approach using orthotropic damage mechanics to describe the concrete behavior. The model, based on the effective stresses concept and the existence of self-stresses at paste-aggregate interfaces, has the following main features: description of the orthotropy induced by cracks (in tension as well as in compression), ability of progressive rotation of the damage eigendirections (in function of those of stress tensor), description of the unilateral aspect, reproduction of anisotropic strains due to cracks opening. The two 2nd order damage tensors, corresponding to direct tension and compression, are deduced from the damage states by the theory of the weakest link. An original method allows to generalize this theory in the cases of non-radial loadings, and can be extended to other causes of degradation (chemical attacks for example). The model is implemented in the case of plane stresses in the finite elements code CASTEM 2000, developed at CEA. Several numerical simulations are then presented. The produced results show a satisfactory description of rotations of eigendirections of the damage tensors consecutive to a progressive rotation of the loading directions. In addition, simulations of two types of notched beams are carried out. The numerical results obtained are confronted with experimental data, and this comparison shows that the model describes in a precise and reliable way the main aspects and phenomena underlined by the tests. The scale effect is correctly reproduced on the three notched beams of different size; in the same way the numerical results obtained on the Iosipescu beam show a good description of the damage facies and a satisfactory agreement in term of crack opening.

An extension of this model coupling chemical and mechanical degradations (alkali-aggregate reaction) is in progress. In addition, the numerical implementation of the model in 3D formulation is in project.

5 ACKNOWLEDGMENTS:

EDF/CIH is gratefully acknowledged for its financial support. CEA/DMT/SEMT/LAMS is also thanked for providing the finite elements code CASTEM 2000.

6 BIBLIOGRAPHY

- Bary, B., Bournazel, J.P., Bourdarot, E. 2000. A poro-damage approach applied to hydro-fracture analysis of concrete. *J. of Eng. Mech.* Vol. 126 (9): 937-943.
- Bazant, Z. P., Planas, J. 1998. *Fracture and Size Effect in Concrete and Other Quasibrittle Materials*. CRC Press.
- Feenstra, P. H., De Borst, R. 1995. Plasticity model and algorithm for mode-I cracking in concrete. *International Journal for Numerical Methods in Engineering*, Vol. 38 (15): 2509-2529.
- Fichant, S., Pijaudier-Cabot, G., La Borderie, C. 1997. Continuum damage modeling: approximation of crack induced anisotropy *Mechanics Research Communications*. Vol. 24 (2): 109-114.
- Hillerborg, A., Modeer, M., Petersson, P. E. 1976. Analysis of crack formation and crack growth in concrete by means of fracture mechanics and finite elements. *Cement and Concrete Research*, Vol. 6: 773-782.
- Mazars, J., Berthaud, Y., Ramtani, S. 1990. The unilateral behaviour of damaged concrete. *Eng. Frac. Mech.*, Vol. 35 (4): 1669-1673.
- Oliver, J. 1989. A consistent characteristic length for smeared cracking model. *Int J. Numer. Method in Engrg.* Vol. 28: 461-474.
- Van Mier, J.G.M. 1984. Strain-Softening of concrete under Multiaxial Loading Condition *PHD thesis* Eindhoven University of Technology, Eindhoven, The Netherlands,
- Schlengen, E. 1993. Experimental and numerical analysis of fracture processes in concrete, *Dissertation*, Delft University of Technology.
- Saouridis, C. 1988. Identification et numérisation objective des comportements adoucissants : une approche multi-échelle du comportement du béton. *PhD thesis* (in french). Univ. Paris VI.
- Sellier, A., Capra, B., Mébarki, A. 1999. Concrete behaviour : a probabilistic damage model. *Proc. of ICASP8**99 (Sydney)*: 331-336 Rotterdam:Balkema.
- Tandon, S., Faber, K.T., Bazant, Zdenek P., Li Yuan, N. 1995. Cohesive crack modeling of influence of sudden changes in loading rate on concrete fracture. *Engineering Fracture Mechanics*. Vol. 52(6): 987-997.
- Weibull, A. 1936. Statistical theory of the strenght of material. *Proc Royal Swedish Inst for Engineering research*: 139-151
- Zienkiewicz, O. C., Taylor, R. L. 1986. *The finite element method*. Mc Graw-Hill.